Steady State Relation between Cytoplasmic Free Ca^{2+} Concentration and Force in Intact Frog Skeletal Muscle Fibers

Masato Konishi and Masaru Watanabe

From the Department of Physiology, The Jikei University School of Medicine, Tokyo 105, Japan

ABSTRACT The steady state relation between cytoplasmic Ca^{2+} concentration ($[Ca^{2+}]_i$) and force was studied in intact skeletal muscle fibers of frogs. Intact twitch fibers were injected with the dextran-conjugated Ca^{2+} indicator, fura dextran, and the fluorescence signals of fura dextran were converted to $[Ca^{2+}]_i$ using calibration parameters previously estimated in permeabilized muscle fibers (Konishi and Watanabe. 1995. *J. Gen. Physiol.* 106:1123–1150). In the first series of experiments, $[Ca^{2+}]_i$ and isometric force were simultaneously measured during high K^+ depolarization. Slow changes in $[Ca^{2+}]_i$ and force induced by 15–30 mM K^+ appeared to be in equilibrium, as instantaneous $[Ca^{2+}]_i$ versus force plot tracked the common path in the rising and relaxation phases of K^+ contractures. In the second series of experiments, 2,5-di-*tert*-butylhydroquinone (TBQ), an inhibitor of the sarcoplasmic reticulum Ca^{2+} pump, was used to decrease the rate of decline of $[Ca^{2+}]_i$ after tetanic stimulation. The decay time courses of both $[Ca^{2+}]_i$ and force were dose-dependently slowed by TBQ up to 5 μM; the instantaneous $[Ca^{2+}]_i$–force relations were nearly identical at ≥1 μM TBQ, suggesting that the change in $[Ca^{2+}]_i$ was slow enough to reach equilibrium with force. The $[Ca^{2+}]_i$–force data obtained from the two types of experiments were consistent with the Hill curve using a Hill coefficient of 3.2–3.9 and $[Ca^{2+}]_i$ for half activation (Ca_{50}) of 1.5–1.7 μM. However, if fura dextran reacts with Ca^{2+} with a 2.5-fold greater K_d as previously estimated from the kinetic fitting (Konishi and Watanabe. 1995. *J. Gen. Physiol.* 106:1123–1150), Ca_{50} would be 3.7–4.2 μM. We also studied the $[Ca^{2+}]$–force relation in skinned fibers under similar experimental conditions. The average Hill coefficient and Ca_{50} were estimated to be 3.3 and 1.8 μM, respectively. Although uncertainties remain about the precise levels of $[Ca^{2+}]_i$, we conclude that the steady state force is a 3rd to 4th power function of $[Ca^{2+}]_i$, and Ca_{50} is in the low micromolar range in intact frog muscle fibers, which is in reasonable agreement with results obtained from skinned fibers.

KEY WORDS: Ca^{2+}–force relation • skinned fibers • K contracture • an inhibitor of sarcoplasmic reticulum • fura dextran

INTRODUCTION

In skeletal muscle, an increase in cytoplasmic free Ca^{2+} concentration ($[Ca^{2+}]_i$)[1] initiates muscle contraction to generate force. The steady state relation between the free Ca^{2+} concentration ($[Ca^{2+}]$) and force has been extensively studied with skinned fibers in which the cell membrane is removed either mechanically or chemically (Natori, 1954; Endo and Iino, 1980), allowing direct control of $[Ca^{2+}]$ in the myofibrillar space. A disadvantage of skinned fibers, however, is that myofibrils are exposed to an artificial environment; the lack of accurate information on cytoplasmic constituents makes it difficult to design bathing solutions for skinned fibers that mimic concentrations of all ions and other constituents found in the cytoplasm of intact muscle fibers. Thus, some quantitative aspects of the $[Ca^{2+}]$–force relation obtained from skinned fibers may not be valid in intact muscle fibers.

A recent study with intact skeletal muscle fibers of frogs reported a very steep $[Ca^{2+}]_i$–force relation (Morgan et al., 1997); a small increase in $[Ca^{2+}]_i$ of 17–32% (i.e., decrease in pCa of 0.07–0.12) could increase the generated force level from 10 to 90% of maximum force. From the fitted Hill curve, they obtained a Hill coefficient (the slope factor) of 15–25, which is much higher than the 2–5 range generally reported with skinned fibers (e.g., Godt and Lindley, 1982; Stephenson and Williams, 1985; Maughan et al., 1995). Hill coefficients of 15–25 are also much higher than other estimates in intact skeletal muscle fibers either from mice (5.1; Westerblad and Allen, 1993) or from *Xenopus* (4.1; Westerblad et al., 1997). In intact cardiac trabeculae, Hill coefficients of 4–6 were found using tetanized preparations (Yue et al., 1986; Okazaki et al., 1990; Gao et al., 1994), and the Hill coefficient was significantly

Portions of this work were previously published in abstract form (Konishi, M., M. Watanabe, and S. Kurihara. 1995. *J. Muscle Res. Cell Motil.* 16:346; Konishi, M., M. Watanabe, and S. Kurihara. 1996. *Jpn. J. Physiol.* 45:S85).

Address correspondence to Dr. Masato Konishi, Department of Physiology, The Jikei University School of Medicine, 3-25-8 Nishishinbashi, Minato-ku, Tokyo 105, Japan. Fax: 81-3-3433-1279; E-mail: konishi@jikei.ac.jp

[1] *Abbreviations used in this paper:* AM, acetoxy-methyl; $[Ca^{2+}]_i$, cytoplasmic free Ca^{2+} concentration; R, ratio signal; SR, sarcoplasmic reticulum; TBQ, 2,5-di-*tert*-butylhydroquinone or 2,5-di(*tert*-butyl)-1,4-benzohydroquinone.

decreased after skinning the intact preparations (Gao et al., 1994).

Because estimation of the $[Ca^{2+}]_i$–force relation in intact preparations generally relies on measurement of $[Ca^{2+}]_i$ with optical indicators, accurate calibration of the indicator signals in terms of $[Ca^{2+}]_i$ is critical. It has been recognized that Ca^{2+} indicator molecules are bound to cellular constituents within the cytoplasm, and this binding alters both spectral and Ca^{2+} binding properties of the indicators (Beeler et al., 1980; Konishi et al., 1988; Kurebayashi et al., 1993; Baker et al., 1994). The methodological difficulties in calibrating indicator signals introduces significant uncertainty about the estimated levels of $[Ca^{2+}]_i$, and consequently the $[Ca^{2+}]_i$–force relation. Despite differences in muscle type and in animal species, large discrepancies in the estimates of the Hill coefficients may be related to calibration difficulties.

To resolve this important uncertainty about the steady state relation between $[Ca^{2+}]_i$ and force in intact muscle fibers, we used fura dextran, fura-2 conjugated to high molecular weight dextran (mol wt ≈ 10,000), to monitor $[Ca^{2+}]_i$. Calibration parameters estimated in the fiber interior were used to convert the indicator fluorescence ratio signals to $[Ca^{2+}]_i$, as previously described (Konishi and Watanabe, 1995). The steady state $[Ca^{2+}]_i$–force relation was constructed by plotting slowly changing $[Ca^{2+}]_i$ versus isometric force simultaneously measured during K^+ contractures and during the relaxation phase of tetani with inhibited sarcoplasmic reticulum (SR). We also constructed conventional $[Ca^{2+}]$–force relation in skinned fibers with many experimental conditions matched to those of intact fiber experiments. The results obtained from intact fibers using two different protocols and from skinned fibers with a conventional method are compared.

METHODS

Intact Muscle Fibers

Single muscle fibers dissected from the anterior tibialis muscle of *Rana temporaria* were mounted in the narrow trough (3 mm width, 3 mm depth, and 50 mm length) of the experimental chamber, and perfused with a continuous flow of normal Ringer's solution. The fiber was stretched to sarcomere length of 2.6–2.8 μm between a fixed hook and the arm of a force transducer (BG-10; Kulite Semiconductor Products, Inc., Leonia, NJ) via small tungsten hooks tied with silk thread to the tendon ends. Sarcomere length of the resting fiber was measured from the first order laser diffraction lines (He/Ne, 5 mW; NEC Corp., Tokyo, Japan), and occasionally checked during the course of the experiments. Even with fixed tendon ends, sarcomeres are somewhat shortened as the force increases and extends the tendons (Huxley and Simmons, 1970). To decrease extra end compliance, and to reduce the movement artifact during fiber activity in the fluorescence records, the fiber was moderately stretched to a resting sarcomere length of 2.6–2.8 μm. Further stretch to longer sarcomeres (>3 μm), on the other hand, causes inhomogeneity of the sarcomeres within the fiber (Huxley and Peachy, 1961), and makes the meaningful comparison between the indicator fluorescence signal and force difficult; fluorescence signals are measured in the middle of the fiber, where sarcomeres are longer and generate less force than those near the tendon ends.

The fibers were electrically stimulated by a 0.5-ms pulse of 1.5× threshold through a pair of platinum-black electrodes running parallel to the whole length of the fiber. The fiber condition was occasionally checked during the experiments by applying a tetanic stimulation (50 Hz for 1 s or 100 Hz for 0.5 s); the experiment was terminated if the fiber did not show sustained plateau tension. The temperature of the perfusing solutions was monitored and set at 17.0 ± 0.5°C.

The normal Ringer's solution contained (mM): 115 NaCl, 2.5 KCl, 1.8 $CaCl_2$, and 5 MOPS, pH 7.15 (17°C). To raise extracellular K^+ concentration ($[K^+]_o$) to 15–100 mM, high K^+ solutions of constant $[K^+] \times [Cl^-]$ product (303 mM^2) were prepared by equimolar substitution of NaCl with K-methanesulfonate and Na-methanesulfonate (see Luttgau and Spiecker, 1979). 2,5-di-*tert*-butylhydroquinone or 2,5-di(*tert*-butyl)-1,4-benzohydroquinone (TBQ) obtained from Tokyo Kasei Organic Chemicals (Tokyo, Japan) was dissolved in normal Ringer's solution from a 100-mM stock solution in DMSO. Tetrodotoxin was from Sankyo Co. Ltd. (Tokyo, Japan). The same lot of fura dextran (potassium salt; 1.0 dye/molecule; mol wt ≈ 10,000) as used in a previous study (Konishi and Watanabe, 1995) was purchased from Molecular Probes, Inc. (lot 2921; Eugene, OR) and used throughout the study.

Fluorescence Recording Procedures

The apparatus and methods for fluorescence measurements have been described previously (Konishi et al., 1993; Konishi and Watanabe, 1995). Briefly, two excitation light beams of different wavelengths were switched at 100 Hz–1 kHz (f_e), and the emitted fluorescence at 500 nm (40 nm FWHM) was sampled at 20 Hz–1 kHz (f_s) with an eight-pole Bessel low-pass filter at 20 Hz–2 kHz (f_c). For the long time-base recordings (∼200 s, high K^+ exposure), f_e, f_s, and f_c were set to 100, 20, and 20 Hz, respectively. Low-pass filtering at 20 Hz should little distort the slow fluorescence signals induced by $K^+ \leq 30$ mM with time to half peak ∼3 s or longer (see Fig. 2), which were primarily analyzed in the present study. For the recordings during normal tetani, on the other hand, the f_e, f_s, and f_c were 1 kHz, 1 kHz, and 500 Hz, respectively. When the time course of tetani was prolonged by inhibition of the SR Ca^{2+} pump, f_s was reduced to 500–200 Hz to extend the sampling period up to 50 s.

For the excitation wavelengths (5 nm FWHM), we chose 360 nm (an isosbestic wavelength for Ca^{2+}) and 382 nm (the wavelength at which the fluorescence change by Ca^{2+} is maximal) (Konishi and Watanabe, 1995). The ratio of the fluorescence intensities excited at 382 nm [F(382)] and 360 nm [F(360)] was converted to $[Ca^{2+}]_i$. Slow drift of the optical instruments (e.g., aging of the lamp) was seen during the course of the study, and was corrected by occasional measurement of the fluorescence ratio signal (R) in the Ca^{2+}-free calibration solution (below) as a standard; all measured values of R were normalized to the standard R value taken with the identical optics. In calibration solutions, the normalized R value lies between 1.0 (Ca^{2+} free) and 0.08 (Ca^{2+} bound).

In Vitro Fluorescence Measurements

Effects of TBQ on fura dextran were examined in quartz capillaries (i.d. ≈ 150 μm; Vitro Dynamics Inc., Rockaway, NJ) filled with buffer solutions containing 25 μM fura dextran. The capillaries were placed in the muscle chamber, and the fluorescence R was measured at five different $[Ca^{2+}]$'s between 0 and 47 μM. The

buffer solution contained 0–10 mM $CaCl_2$, 10 mM EGTA, 1 mM free Mg^{2+}, and 20 mM PIPES (pH 7.0); ionic strength was adjusted to 0.15 M by K-methanesulfonate. In the calculation of free concentrations of Ca^{2+} and Mg^{2+}, the apparent dissociation constants of EGTA for Ca^{2+} and Mg^{2+} were assumed to be 0.41 μM and 47 mM, respectively, based on the equilibrium constants given by Martell and Smith (1974). TBQ (5 μM) did not cause a significant change in R at any given $[Ca^{2+}]$ level, nor in the estimated Ca^{2+} dissociation constant of fura dextran (which was 0.54 and 0.55 μM in the absence and presence of TBQ, respectively).

In Vivo Fluorescence Measurements

At the beginning of each experiment, the background fluorescence was measured from the fiber in the absence of indicator. Fura dextran was dissolved in the buffer solution (100 mM KCl, 2 mM PIPES, pH 7.0) at a concentration of 5 mM, and was pressure injected into the muscle fiber. Diffusion of fura dextran along the fiber axis was allowed for at least 30 min after injection, before the first fluorescence measurement. The indicator fluorescence in the cytoplasm was calculated, at each wavelength, by subtraction of the background fluorescence from the total fluorescence intensity measured in the same portion of the muscle fiber. Spatially averaged fura dextran concentration in the cytoplasm was estimated, as previously described (Konishi and Watanabe, 1995), from the F(360) measured in the fiber, and was at most 91 μM in the 22 fibers used in the present study. It has been shown that $[Ca^{2+}]_i$ at rest and during activity was not altered by the Ca^{2+} buffering with an indicator concentration of ~100 μM or lower (Konishi and Watanabe, 1995).

Since 360 nm is an isosbestic wavelength of fura dextran for Ca^{2+}, any change in F(360) during muscle activity may be attributed to fiber movement. Although the moderate stretching of the fiber helped to reduce the fiber movement, there often remained significant movement artifact in the fluorescence records. Large fiber movement might move the fiber out of focus, and might distort the Ca^{2+}-related fluorescence signal, even though the fluorescence ratio was employed. We therefore did not include the data in the analysis, if the change in F(360) was greater than 10% of the resting level (see legend to Fig. 3).

In the absence of any distortion due to fiber movement, the fluorescence ratio signal should lie between R_0 and R_1, the R at 0 $[Ca^{2+}]_i$ and saturating $[Ca^{2+}]_i$, respectively, and should be linearly related to the Ca^{2+}-bound fraction of the indicator (f_{CaD}):

$$f_{CaD} = (R - R_0) / (R_1 - R_0). \quad (1)$$

f_{CaD} can then be converted to $[Ca^{2+}]_i$ with an equation of the form:

$$[Ca^{2+}]_i = \frac{df_{CaD}/dt + f_{CaD} \cdot K_{-1}}{(1 - f_{CaD})\, K_{+1}}, \quad (2)$$

where K_{+1} and K_{-1} denote the indicator's association and dissociation rate constants, respectively, for Ca^{2+}. K_d is defined as K_{-1}/K_{+1}. In the steady state, Eq. 2 can be simplified to yield the standard equation:

$$[Ca^{2+}]_i = K_d \frac{f_{CaD}}{1 - f_{CaD}}. \quad (3)$$

In most of the present study, Eq. 3 was used, assuming that the kinetics of Ca^{2+}-fura dextran reaction were fast enough to follow changes of $[Ca^{2+}]_i$ to be analyzed. For the three calibration parameters (R_0, R_1, and K_d), values previously estimated in permeabilized muscle fibers were used; $R_0 = 1.105$, $R_1 = 0.106$ (1.105×0.096), and $K_d = 1.0$ μM (Konishi and Watanabe, 1995). In some analyses, however, kinetic correction was included based on Eq. 2; K_{-1} was assumed to be 80 s^{-1}, an average value estimated in the previous study (Konishi and Watanabe, 1995). K_{+1} was set to 8×10^7 M^{-1} s^{-1} to be consistent with K_d (K_{-1}/K_{+1}) of 1.0 μM (above). Note that the waveform of calculated $[Ca^{2+}]_i$ depends only on K_{-1}; K_{+1} determines the amplitude as a scaling factor (see Eq. 2).

To estimate the upper detection limit of $[Ca^{2+}]_i$ in intact fibers, two experiments were carried out on a highly stretched fiber (resting sarcomere length 3.8 μm) stimulated by a train of action potentials in the presence of 10 μM TBQ, an inhibitor of SR Ca^{2+} pump (Fig. 1). Because these fibers were well immobilized, movement artifact on the R signal, if any, was considered to be minor. In the fiber shown in Fig. 1 and the other fiber, tetanic stimulation (67 or 50 Hz) in the presence of 10 μM TBQ caused a large decrease in R to, on average, 0.152. This R value, if calibrated as described above, corresponds to the indicator's Ca^{2+}-bound fraction of 0.954 or 20.7 μM $[Ca^{2+}]_i$ (4.68 in pCa unit). It is therefore suggested that the indicator R signal does not sensitively reflect $[Ca^{2+}]_i$, if $[Ca^{2+}]_i$ level approaches this level. Note that the most important part of the pCa–force relation presented in RESULTS lies in pCa 5–6, within the sensitive range of the indicator.

Experimental Protocol

Two experimental maneuvers were employed to induce slow changes in $[Ca^{2+}]_i$ and force.

(*a*) *Depolarization by high* $[K^+]_o$. Solutions of constant $[K^+] \times [Cl^-]$ product were exchanged with relatively fast flow; the velocity in the trough was 3–9 cm/s. Before each application of high

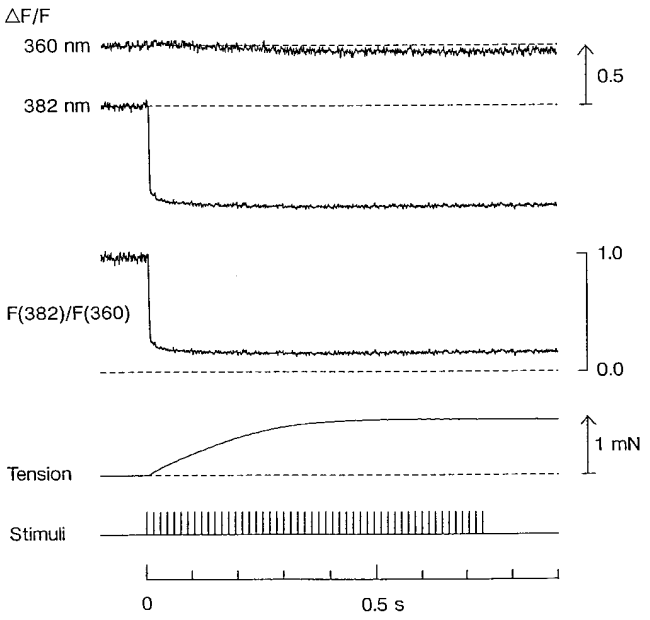

FIGURE 1. Fura dextran fluorescence and force records during high frequency stimulation in the presence of 10 μM TBQ. The muscle fiber was incubated in Ringer's solution containing 10 μM TBQ for 25 min. Fluorescence changes (ΔF) with excitation at 360 and 382 nm (*first* and *second traces*) were normalized to the resting fluorescence level (F) at each wavelength, and are displayed as fractional changes (ΔF/F). The third trace is the fluorescence ratio R, and the fourth trace shows tetanic force. The bottom trace shows 50 stimuli (width 500 μs, interval 15 ms). Fiber, 112793f2; resting sarcomere length, 3.8 μm; indicator concentration, 91 μM.

K^+ solution, the fiber was pretreated with 3 μM tetrodotoxin (in the normal Ringer's solution) for 2 min; inhibition of action potential generation was indicated by lack of twitch in response to single electrical stimulation. High $[K^+]_o$ applications were separated by a recovery period of at least 25 min, during which the fiber was perfused with normal Ringer's solution to completely restore the resting levels of $[Ca^{2+}]_i$.

(*b*) *Tetani in the presence of TBQ.* $[Ca^{2+}]_i$ and force were recorded with high frequency stimulation (100 Hz for 0.5 s) in the absence and presence of 0.2–5 μM TBQ. In each run, the fiber was kept in the resting state during a 10-min treatment with TBQ before the tetanic stimulation. After recording fluorescence and force with the tetanic stimulation, the fiber was perfused with normal Ringer's solution for 5–15 min before a new run was started. Experiments began with a control tetanus in the absence of TBQ, and TBQ concentration was gradually increased for the following runs. At the end of some experiments (7 of 11 fibers), the fiber was thoroughly washed with the normal Ringer's solution for 30–60 min, and a tetanus was induced in the absence of TBQ.

Skinned Fiber Experiments

Single fibers (also isolated from the anterior tibialis muscle of *Rana temporaria*) were treated with 1% triton X-100 in the relaxing solution (below) for 30 min to remove the cell membrane and membranes of intracellular organelles (e.g., SR and mitochondria). One end of the skinned segment (several millimeters in length) was tied with a silk monofilament to a tension transducer (BG-10; Kulite Semiconductor Products) and the other end was tied to a fixed hook. Resting sarcomere length was initially set to 2.7–2.8 μm by observation of the first order laser diffraction lines. The apparatus for force measurements in skinned fibers has been described previously (Horiuti et al., 1988). A plastic plate with 15 wells (0.5 ml in volume) was used. The fiber was soaked in one of the solutions in the wells with continuous stirring. The solution surrounding the fiber was quickly changed by the sliding motion of the plate, which transferred the fiber between wells. Temperature of solutions in the wells was kept at 16–18°C by a thermobath attached underneath the plate.

All the solutions for skinned fiber experiments contained in common (mM) 1.0 free Mg^{2+}, 4.0 MgATP, 10.0 creatine phosphate, 10.0 EGTA, 10.0 PIPES, pH 7.0 by KOH. Solutions of various $[Ca^{2+}]$'s were prepared by mixing a solution containing 10 mM EGTA with no Ca^{2+} (relaxing solution) and a solution containing 10 mM EGTA plus 10 mM Ca^{2+}. Solution $[Ca^{2+}]$ in the present experimental condition (pH 7.0, 17°C) was calculated by solving simultaneous equations using the equilibrium constants listed by Martell and Smith (1974), as previously described (Horiuti et al., 1988; Konishi and Watanabe, 1995; also see above for the apparent dissociation constants of EGTA). K-methanesulfonate was added to maintain the ionic strength at 0.15 M. Leupeptin (10 μM; Sigma Chemical Co., St. Louis, MO) was also included to inhibit Ca^{2+}-activated proteases. EGTA (Nakalai Tesque Inc., Kyoto, Japan), Ca-methanesulfonate (Tokyo Kasei Organic Chemicals), Na_2ATP (Boehringer Mannheim GmbH, Mannheim, Germany), and creatine phosphate (disodium salt or dipotassium salt; Sigma Chemical Co.) were of the highest analytical grade. No obvious difference in the pCa–force relation was observed by the choice of disodium salt or dipotassium salt of creatine phosphate.

The fiber was activated by sequential changes of solutions with various $[Ca^{2+}]$ from 0.32 μM (pCa 6.5) to 40 μM (pCa 4.4), and was then allowed to relax in the relaxing solution. To compensate for fiber deterioration (decrease in force), the pCa run was repeated three times with ~15-min intervals in each fiber.

Data Processing and Analysis

Records of $[Ca^{2+}]_i$ and force obtained from intact fibers were smoothed with quadratic polynomial curve fitting to 15 points (a central point and 7 points on both sides) to reduce noise. This smoothing did not affect the general time course of either $[Ca^{2+}]_i$ or force during K^+ contractures and tetani, but slightly distorted $[Ca^{2+}]_i$ transients during twitches; with 1-kHz sampling, the peak amplitude was reduced by ~10% and time to peak was prolonged by ~2 ms.

Nonlinear least-squares fitting analysis was carried out with a program that uses Gauss-Newton algorithm. The $[Ca^{2+}]$–force data obtained in either intact or skinned fibers were fitted with a Hill equation:

$$\text{Force} = \text{Force}_{max} \frac{[Ca^{2+}]^N}{Ca_{50}{}^N + [Ca^{2+}]^N}, \quad (4)$$

where Force_{max} and Ca_{50} denote, respectively, maximum force and $[Ca^{2+}]$ that gives half maximal force. N (Hill coefficient) is a measure of the slope.

Results obtained from more than two repeated experiments are reported as means ± SEM. Statistical significance was tested using the two-tailed *t* test, with the significance level set at $P < 0.05$.

RESULTS

Fluorescence and Force Measurements with Increased $[K^+]_o$

The average level of resting $[Ca^{2+}]_i$ measured at normal $[K^+]_o$ (2.5 mM) was 0.060 ± 0.003 μM ($n = 22$) in the present study, which was similar to the previously reported value (0.055 μM; Konishi and Watanabe, 1995). The increase in $[K^+]_o$ from 2.5 to 10 mM caused a slight but significant increase in $[Ca^{2+}]_i$ to 0.070 ± 0.002 μM ($n = 7$; paired *t* test) without detectable force generation. A further increase in $[K^+]_o$ to 15 mM caused a much larger increase in $[Ca^{2+}]_i$ to 0.268 ± 0.077 μM ($n = 8$) (see Fig. 2 *A*). At 15 mM $[K^+]_o$, force generation was not generally observed except for one fiber, in which a large increase in $[Ca^{2+}]_i$ to 0.77 μM was accompanied by development of a small force (~2% of tetanic force). The threshold for the force generation appeared to be 15–20 mM $[K^+]_o$, because all fibers tested showed clear active force (5–60% of tetanic force) at 20 mM $[K^+]_o$ with $[Ca^{2+}]_i$ levels raised to 0.74–2.02 μM ($n = 9$).

Fig. 2 shows an example of the experiment in which $[Ca^{2+}]_i$ and force measurements were repeated at various $[K^+]_o$ (10–100 mM) in a single fiber (results at 10 mM $[K^+]_o$ are not shown). In this fiber, 15 mM $[K^+]_o$ caused a slow and slight decrease of the fluorescence R signal (i.e., increase of $[Ca^{2+}]_i$) without detectable force (Fig. 2 *A*). The slight decrease in F(360) could be attributed to photobleaching of the indicator due to prolonged illumination. Changes in the fluorescence R signal and force were clearly observed at 20 mM $[K^+]_o$ (Fig. 2 *B*), and were further enhanced at 30 (*C*) and 100 (*D*) mM $[K^+]_o$. At 100 mM $[K^+]_o$, development of a large force introduced significant movement artifact in the F(360) record (Fig. 2 *D, arrow*); we could not reliably

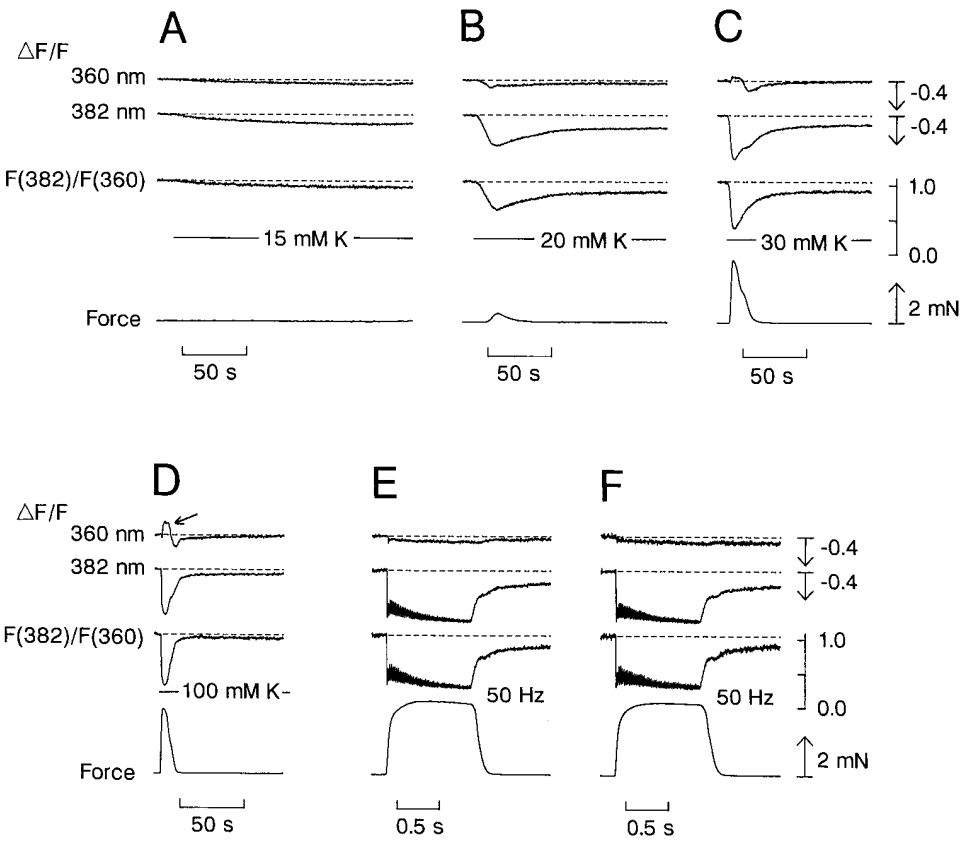

FIGURE 2. The fluorescence signals of fura dextran and force recorded during exposure to high K^+ (*A–D*) or 50 Hz tetanic stimulation (*E* and *F*). In *A–F*, the top two traces are the fractional changes in the fluorescence intensity at indicated wavelengths relative to the resting level at each wavelength (ΔF/F). The third trace is the fluorescence ratio R. The fourth trace shows force. For *A–D*, the K^+ concentration is indicated in each panel. Records were taken in sequence of *E, A, B, C, D,* and *F* from a fiber. Fiber, 050694f1; resting sarcomere length, 2.7–2.8 μm; 41–17 μM indicator. For prolonged time-base recordings during high K^+ exposure (*A–D*), a neutral density filter (FDU-0.5; OFR Co., Caldwell, NJ) was inserted into the optical path of the excitation light beam to minimize photobleaching of the indicator. This filter causes nearly equal reduction of F(382) and F(360) to ~30%, and thus causes only a 0.4% change in the standard R.

measure the fluorescence signals [$\Delta F(360)/F(360) \leq 0.1$, see METHODS] in any of three fibers tested at 100 mM $[K^+]_o$. Fiber movement was often a problem even at 30 mM $[K^+]_o$. In Fig. 2 *C*, a relatively large movement artifact [downward change in $\Delta F(360)/F(360)$] was observed ~14 s after application of 30 mM $[K^+]_o$; only the earlier part of these fluorescence signals were analyzed.

During the K^+ contracture experiment, occasional application of a tetanic stimulation (50 Hz for 1 s) produced a nearly complete fusion of force to form a plateau in the present experimental conditions (Fig. 2, *E* and *F*). Because $[Ca^{2+}]_i$ and force are thought to be in equilibrium in the plateau phase, additional information on the steady state relation between $[Ca^{2+}]_i$ and force could be obtained; the records of fluorescence R and force in the plateau phase were analyzed in the following sections. After the end of tetanic stimulation, rapid return of the fluorescence R was followed by a slower fall in force. We occasionally observed a "bump" in the return phase of the fluorescence R (see Fig. 2, *E* and *F*). This bump may reflect the secondary rise of $[Ca^{2+}]_i$, which has been reported with other indicators (Cannell, 1986; Lee et al., 1991; Caputo et al., 1994), although it could also be attributed to a small correction error for the fiber movement. We did not further study the bump in the present study.

The fluorescence R and force during tetani were very similar at the beginning (Fig. 2 *E*), in the middle (not shown), and at the end (Fig. 2 *F*) of the high K^+ runs (Fig. 2, *A–D*). Resting $[Ca^{2+}]_i$ was also unchanged; 0.059 μM at the beginning (Fig. 2 *E*) and 0.058 μM at the end (Fig. 2 *F*) of the experiment. Thus, the fiber conditions appeared to be well maintained throughout the experiment.

$[Ca^{2+}]_i$–Force Relation during K^+ Contractures

Fig. 3 *A* plots peak $[Ca^{2+}]_i$–peak force data obtained, as described above, from the experiment shown in Fig. 2. The left-most point on the pCa axis (a point at the lowest $[Ca^{2+}]_i$) was obtained in the resting state at normal $[K^+]_o$, and the right-most three points with the largest relative force were obtained during plateau of tetani. The "steady state" $[Ca^{2+}]_i$(pCa)–force relation was described by the Hill curve; a solid line was obtained by least-squares fitting of the filled symbols with parameters shown in Fig. 3 *A*. A similar analysis was carried out for the three other fibers; in four fibers, parameters for the best-fitted Hill curve were $N = 3.92 \pm 0.37$, $Ca_{50} = 1.69 \pm 0.10$ μM and $Force_{max} = 1.014 \pm 0.011$ (Table I).

Because only a limited number of data points could be obtained from single fibers, the results from eight fibers were collected and plotted in Fig. 3 *B*. Fig. 3 *B* shows that these collected data are also reasonably well fitted by the Hill curve with parameters similar to those for individual fibers (Table I).

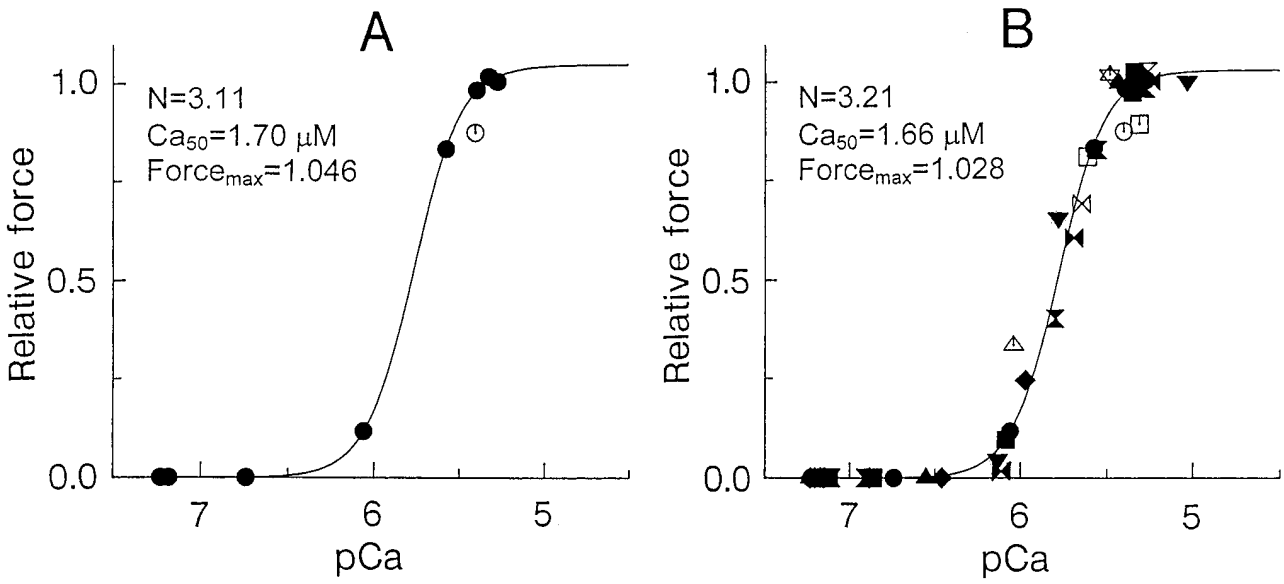

FIGURE 3. The relation between peak $[Ca^{2+}]_i$ (in pCa units) and peak force during high K^+ contractures and tetani. (*A*) Data obtained from a fiber shown in Fig. 2. Two data points that are not shown in Fig. 2 and a point obtained at normal $[K^+]_o$ are also included. (*B*) Pooled data from eight fibers. Each symbol type represents an individual fiber. In *A* and *B*, peak force levels during high K^+ contractures have been normalized to the peak tetanic force in each fiber. (If more than one record of tetanus were available, the average value was set to 1.0.) Filled symbols represent data points that satisfied our criteria for acceptable movement artifact on the fluorescence records [$\Delta F(360)/F(360) \leq 0.1$]. Open symbols are data with larger movement artifact [$\Delta F(360)/F(360) > 0.1$] and are not included in the analysis. Data points are not plotted, if $\Delta F(360)/F(360) > 0.2$. Solid lines represent Hill curves drawn by least-squares fitting to the filled symbols with parameters shown in the panels. Fiber ID, resting sarcomere length, and indicator concentration were as follows: (●, ○) fiber 050694f1, 2.7–2.8 μm, 41–17 μM; (▼) fiber 020194f1, 2.8 μm, 27–15 μM; (▶◀, ▷◁) fiber 021294f1, 2.6 μm, 31–19 μM; (◆, ◇) fiber 050294f1, 2.7–2.8 μm, 68–35 μM; (△, ▲) fiber 050294f2, 2.7–2.8 μm, 42–24 μM; (■, □) fiber 050694f2, 2.7 μm, 51–26 μM; (★, ☆) fiber 051494f2, 2.6 μm, 12–7 μM; (⧗,⧖) fiber 051894f1, 2.6–2.7 μm, 30–16 μM.

The analysis in Fig. 3 assumes that $[Ca^{2+}]_i$ and force are in dynamic equilibrium during slow activation by 10–30 mM $[K^+]_o$, as well as during the plateau phase of tetani. If this is the case, the $[Ca^{2+}]_i$ versus force plot at any times other than that of the peak values should follow the peak relation described above. Each panel of Fig. 4 compares the steady state $[Ca^{2+}]_i$–force relation (*symbols* and *solid curve*) and instantaneous $[Ca^{2+}]_i$ versus force plot during K^+ contractures and plateau of tetani (*dotted lines*) in four fibers. It is clearly seen in each panel that dotted lines do approximately follow the steady state curve during both the rising and the declining phases of K^+ contracture force. Instantaneous plots during plateau of tetani fluctuate around the peaks because of nearly constant levels of $[Ca^{2+}]_i$ and force. Thus, the results shown in Figs. 3 and 4 appear to reflect the steady state relation between $[Ca^{2+}]_i$ and force.

TABLE I

Hill Parameters Estimated in Frog Muscle Fibers (Resting Sarcomere Length 2.6–2.8 μm, 16–18°C)

Type of preparations/measurements	N	Ca_{50}
		μM
Intact fibers		
K^+ contractures		
Individual fibers (n = 4)	3.92 (± 0.37)	1.69 (± 0.10)
Pooled data from eight fibers	3.21	1.66
Tetani with 2 μM TBQ (n = 10)	3.41 (± 0.15)	1.48 (± 0.04)
Skinned fibers (n = 6)	3.25 (± 0.64)	1.81 (± 0.25)

Hill parameters, N and Ca_{50}, were estimated based on least-squares fit of Eq. 4 to data obtained from the experiments shown at left. Each entry gives mean ± SEM from n muscle fibers, except for values from pooled data.

Effects of TBQ on $[Ca^{2+}]_i$ and Force

As another way of producing slow changes in $[Ca^{2+}]_i$, we used TBQ to inhibit SR Ca^{2+} ATPase (Westerblad and Allen, 1994). Fig. 5 shows effects of TBQ (0.2–2 μM) on $[Ca^{2+}]_i$ and force stimulated by a high frequency train (100 Hz, 0.5 s). TBQ dose-dependently enhanced peak $[Ca^{2+}]_i$ without causing much increase in the tetanic force, suggesting that force was nearly saturated at the $[Ca^{2+}]_i$ level achieved during tetanus in the absence of the drug (see also Figs. 3 and 4). TBQ also markedly prolonged the decay of $[Ca^{2+}]_i$ and force after the end of stimulation. These observations are consistent with dose-dependent inhibition of SR Ca^{2+} ATPase by TBQ. Resting $[Ca^{2+}]_i$ just before tetanic stimulation was not significantly altered by TBQ at 1 μM or lower concentrations; in the absence and presence of 1 μM TBQ, average values of resting $[Ca^{2+}]_i$

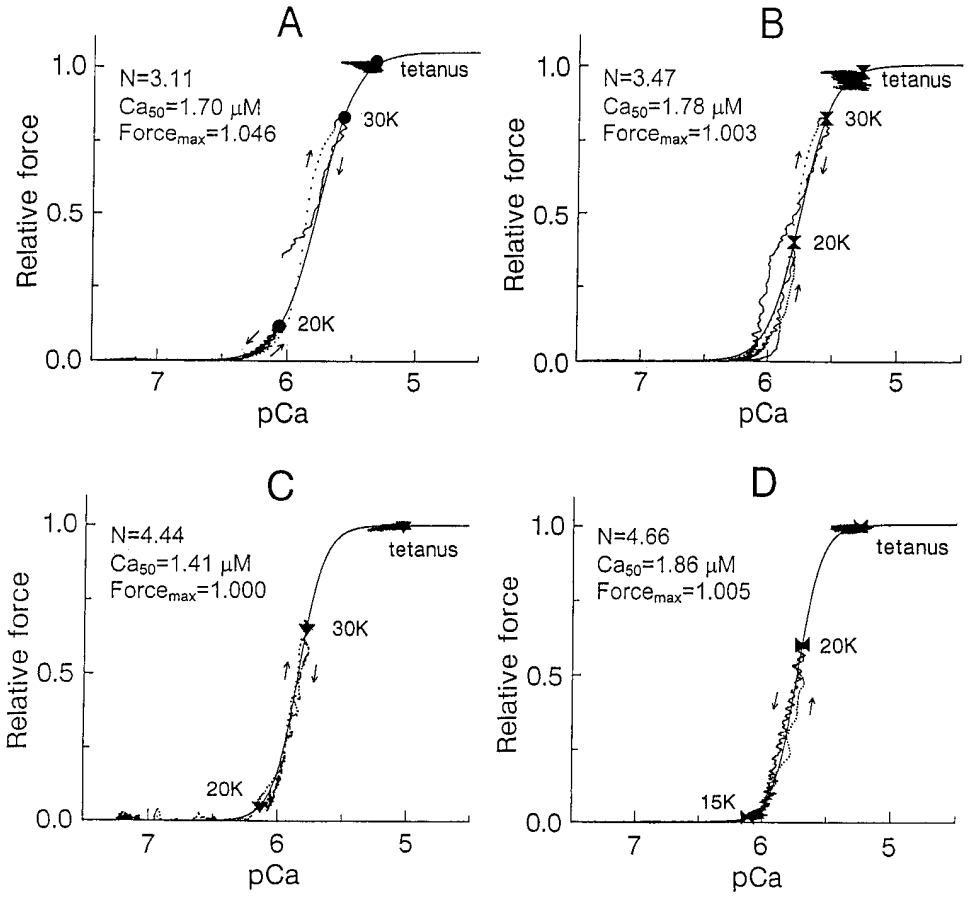

FIGURE 4. $[Ca^{2+}]_i$ (in pCa units) versus force (relative to peak tetanic force) plot obtained in four fibers. Symbols represent peak $[Ca^{2+}]_i$ and peak force during high K^+ contractures (*20K*, 20 mM K^+; *30K*, 30 mM K^+) or tetanus. Solid lines are Hill curves least-squares fitted to the symbols with the best-fitted parameters indicated in the panels. Dotted lines (which appear wavy in some cases) are instantaneous $[Ca^{2+}]_i$ versus force plot during K^+ contractures and plateau phase of tetanus. Arrows indicate the direction of the change as a function of time. (*A*) fiber 050694f1, (*B*) fiber 051894f1, (*C*) fiber 020194f1, (*D*) 021294f1. See legend to Fig. 3 for fiber information.

were 0.056 ± 0.004 and 0.060 ± 0.003 μM, respectively, and these were not statistically different (n = 10, paired t test). Higher concentrations of TBQ caused a slight but significant (paired t test) increase in the resting $[Ca^{2+}]_i$; 0.069 ± 0.004 μM with 2 μM TBQ (n = 10) and 0.071 ± 0.005 μM (n = 8) with 5 μM TBQ. This slight elevation of resting $[Ca^{2+}]_i$ could be due to inhibition of SR Ca^{2+} ATPase, which, in the short term, could counterbalance SR Ca^{2+} leak, but could also result from incomplete recovery from the effect of the preceding tetanus in the presence of TBQ. It seems reasonable to conclude that TBQ (up to 5 μM) does not markedly elevate the resting $[Ca^{2+}]_i$ of unstimulated fibers. The effects of TBQ (at 2–5 μM) were mostly, but not completely, reversed after extensive wash with the normal Ringer's solution for 30–60 min (see Fig. 7, *filled symbols*).

$[Ca^{2+}]_i$ and force records shown in Fig. 5 were plotted on a pCa-force axis (Fig. 6). In contrast to the close similarity between the rising and relaxation phases of K^+ contractures (Fig. 4), data sets from tetani formed counterclockwise loops suggesting nonequilibrium relation between $[Ca^{2+}]_i$ and force either in the rising or the relaxation phase, or both. In the absence of TBQ, the rise of tetanic force probably lags behind $[Ca^{2+}]_i$ because of the delay between Ca^{2+} binding to troponin and the attachment of cross bridges and force generation. TBQ dose-dependently shifted the ascending limb of the loop to the right (Fig. 6), suggesting that the lag between $[Ca^{2+}]_i$ and force was enhanced with a higher rate of rise of $[Ca^{2+}]_i$ in the presence of TBQ. We therefore focused our analysis on the relaxation phase of tetanic force; i.e., the descending limb of the loop. TBQ at relatively low concentrations (0.2 and 0.5 μM) dose-dependently shifted the descending limb to the right (Fig. 6, *top*). However, the increase in TBQ concentration beyond 1 μM did not cause further substantial shift of the descending limb of the loop (Fig. 6, *bottom*).

Fig. 7 summarizes the TBQ concentration-dependent changes in the time courses of $[Ca^{2+}]_i$ and force (assessed by half decay time of $\Delta[Ca^{2+}]_i$ and force), and the shift in the position of the descending limb on the abscissa (assessed by $[Ca^{2+}]_i$ at half relaxation of force). As the decline of $[Ca^{2+}]_i$ and force was slowed by 0.2–1 μM TBQ (Fig. 7, *A* and *B*), the descending limb was shifted towards lower pCa or higher $[Ca^{2+}]_i$ (Fig. 7 *C*). Further prolongation of declining phases of $[Ca^{2+}]_i$ and force by higher concentrations of TBQ (1–5 μM), however, were accompanied by only a slight shift of the descending limb of the loop (Ca_{50} = 1.23 ± 0.04 μM, n = 10; 1.30 ± 0.04 μM, n = 10; and 1.44 ± 0.08 μM, n = 7, at 1, 2, and 5 μM TBQ, respectively). Although the

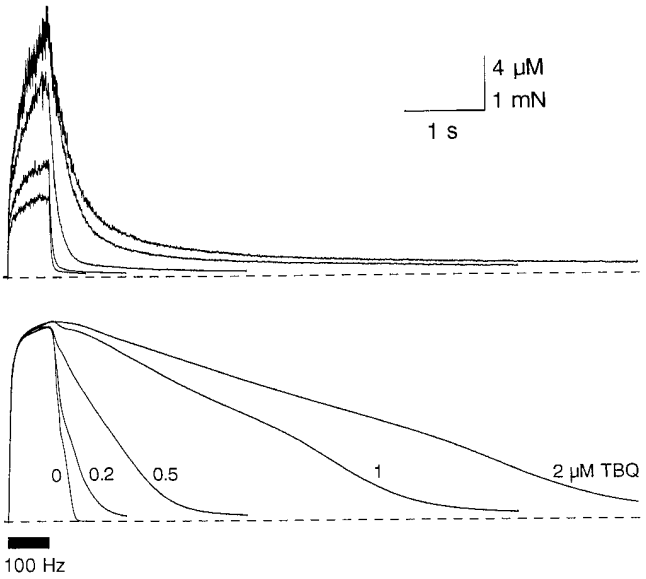

FIGURE 5. Dose-dependent effect of TBQ on changes in $[Ca^{2+}]_i$ (*top*) and force (*bottom*) induced by 100 Hz stimulation (shown below). TBQ concentration was sequentially increased, as indicated near force traces. TBQ dose-dependently slowed the decay phase of $[Ca^{2+}]_i$ and force after secession of stimuli. Fiber 031095f2, resting sarcomere length 2.7–2.8 μm, 90–70 μM indicator concentration.

differences in Ca_{50} were barely significant ($0.01 < P < 0.05$, paired t test), the relatively common descending limb of the loop observed with high concentrations of TBQ (1–5 μM) appears to reflect a near steady state relation between $[Ca^{2+}]_i$ and force.

$[Ca^{2+}]_i$–Force Relation during the Relaxation Phase of Tetani in the Presence of TBQ

Under the assumption that the slow decline of $[Ca^{2+}]_i$ in the presence of high concentrations of TBQ is rate limiting for the relaxation of force, data points sampled from the descending limb of the loop were fitted with the Hill equation (Fig. 8). The fit was generally reasonable, although some displacement was always noticed in the region of relatively high force (>0.7) and high $[Ca^{2+}]_i$ (pCa < 5.7) levels. This displacement was not due to loosening of fiber supports, because some experiments, in which cyanoacrylate glue was used to ensure a firm connection between the tungsten hooks (on both tendon ends) and the two support hooks (the fixed hook and the arm of the force transducer) gave very similar results. Best-fitted values of N and Ca_{50} were 3.40 ± 0.29 and 1.52 ± 0.03 μM, respectively, from four experiments with the glue, and these values were 3.42 ± 0.17 and 1.45 ± 0.07 μM, respectively, from six experiments without the glue. The displacement could be related to internal shortening and lengthening of some sarcomeres (see DISCUSSION), but the underlying mechanism was not further investigated in the present study. In a total of 10 fibers, including

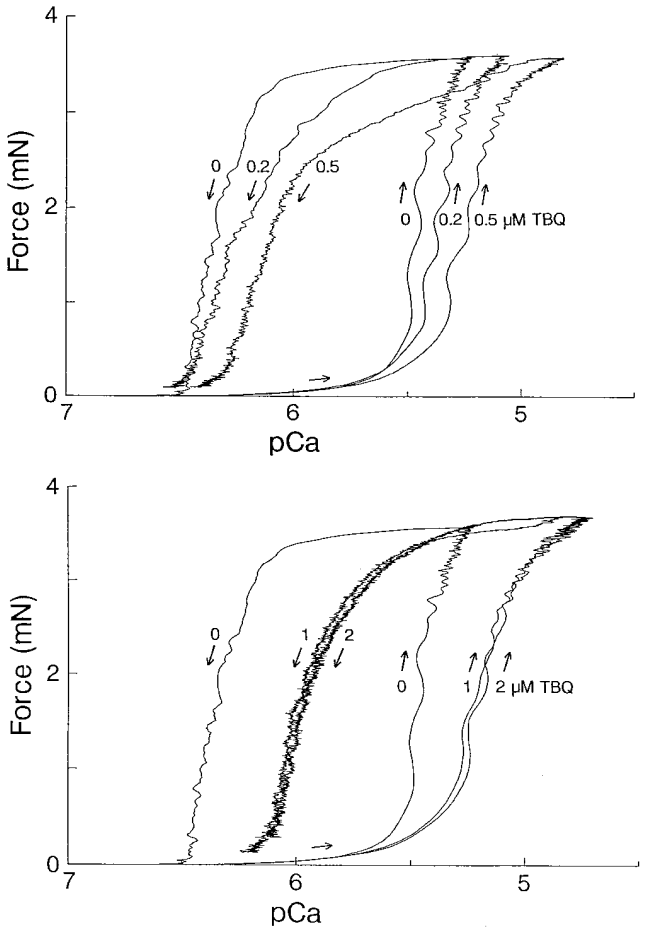

FIGURE 6. Instantaneous plot of $[Ca^{2+}]_i$ (in pCa units) and force during high frequency tetani shown in Fig. 5. (*top*) In the absence (0) and presence of 0.2 and 0.5 μM TBQ. (*bottom*) In the absence (0) and presence of 1 and 2 μM TBQ. Each loop precedes in the direction of arrows.

two fibers shown in Fig. 8, data points in the presence of 2 μM TBQ were best described by the curve with N = 3.41 ± 0.15 and Ca_{50} = 1.48 ± 0.04 μM (Table I).

In the analysis described above, the fluorescence R was converted to $[Ca^{2+}]_i$ using the steady state equation (Eq. 3), assuming that Ca^{2+} binding of fura dextran was in equilibrium with the slow changes in $[Ca^{2+}]_i$ under study. It was therefore important to determine whether the kinetics for the Ca^{2+}-fura dextran reaction would influence the results. Comparison of the results analyzed with or without the kinetic correction (Fig. 9) demonstrates that the kinetic delay of the Ca^{2+}-fura dextran reaction (K_{-1} = 80 s^{-1}) did slightly influence the decay of $[Ca^{2+}]_i$ after control tetanus (Fig. 9 *A*), but did not appreciably change the slow $[Ca^{2+}]_i$ decline in the presence of 2 μM TBQ (Fig. 9 *B*). Similarly, little effect of the kinetic correction on the general time course of $[Ca^{2+}]_i$ was found for all records in the declining phases after tetani in the presence of 1–5 μM TBQ, as well as in K^+ contractures at 15–30 mM $[K^+]_o$

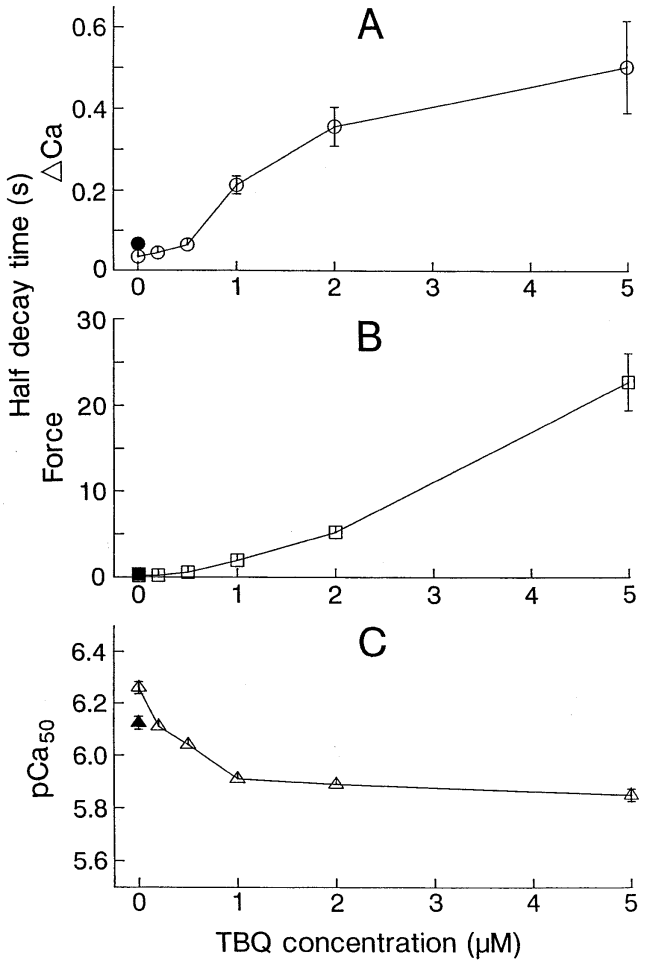

FIGURE 7. Dependence of properties of $\Delta[Ca^{2+}]_i$ and force during tetani on TBQ concentration. (*A*) Time to half decay of $\Delta[Ca^{2+}]_i$ after the last stimulus; (*B*) time to half relaxation of force after the last stimulus; (*C*) $[Ca^{2+}]_i$ level, expressed as pCa units, at the time of half relaxation of force. Symbols represent means ± SEM of data obtained in 7–11 fibers, except for data points at 0.2 μM TBQ ($n = 2$, only mean values are shown). In all experiments, TBQ concentration was sequentially increased. Filled symbols were taken at the end of seven runs, 30–60 min after washout of the highest concentration of TBQ (2 μM in one fiber and 5 μM in six fibers).

(data not shown). Thus, it is unlikely that the kinetic delay of the indicator introduced significant error in the results of the present study.

pCa–Force Relation in Skinned Fibers

A steady state relation between bath $[Ca^{2+}]$ and force was obtained in skinned fibers as shown in Fig. 10, with primary experimental conditions matched to those for intact fibers; skinned fibers of the same muscle type (*m. tibialis anterior*) from the same frog species (*Rana temporaria*) were used at a similar temperature (16–18°C) and resting sarcomere length (2.7–2.8 μm). In freshly prepared preparations, the Hill curve least-squares fitted to data points had $N = 3.25 \pm 0.64$ and $Ca_{50} = 1.81 \pm 0.25$ μM ($n = 6$), which may be compared with those estimated above from intact fibers (Table I).

To determine if TBQ directly influences the Ca^{2+} sensitivity of myofilaments, pCa runs were repeated three times (Fig. 10 *A*). Although some decrease in maximal Ca^{2+}-activated force was noted in the repeated runs (Fig. 10, *A* and *B*), probably due to fiber run-down, N and Ca_{50} were not markedly altered in the three runs (see Fig. 10, *legend*, for N and Ca_{50} values). We therefore averaged the data from the first and third runs (taken in the absence of TBQ) to compare with those in the second run (taken in the presence of 5 μM TBQ) (Fig. 10 *C*). The relative force level at each pCa was not clearly altered by TBQ; only the data points at pCa 5.8 were statistically different ($n = 6$, paired t test). The best-fitted Hill curves for the two data sets were also similar; none of the three parameters were statistically different. Overall, the effect of 5 μM TBQ on myofilament Ca^{2+} sensitivity, if any, appears to be minor (~10% decrease in Ca_{50}), supporting the earlier report in toad skinned fibers (Bakker et al., 1992).

DISCUSSION

In the present study, a comparison of $[Ca^{2+}]_i$ and force simultaneously measured in intact muscle fibers has provided an estimate of the steady state relation between $[Ca^{2+}]_i$ and force. Most information regarding the $[Ca^{2+}]_i$–force relation has been previously obtained from experiments with skinned fibers, in which $[Ca^{2+}]$ around the myofibrils can be precisely controlled. The use of intact fibers has the advantage that the results are clearly of more physiological relevance than those obtained from skinned fibers, but it has the disadvantage that accurate determination of $[Ca^{2+}]_i$ is technically difficult. Because the indicator properties (i.e., optical signals or Ca^{2+} affinity, or both) are, in general, likely altered in the intracellular environment as a result of binding to intracellular macromolecules (Beeler et al., 1980; Konishi et al., 1988; Kurebayashi et al., 1993; Baker et al., 1994), calibration of indicator signals suffers significant uncertainty for $[Ca^{2+}]_i$ both at rest and during activity.

The methodology for measuring $[Ca^{2+}]_i$ employed in the present study was based on the intracellular calibration of fura dextran fluorescence in permeabilized muscle fibers; after the cell membrane was permeabilized by β-escin, calibration parameters, R_0, R_1, and K_d (see Eqs. 1 and 3), were estimated in the fiber interior in the presence of a major fraction of cellular macromolecules; the values estimated were 1.105, 0.106, and 1.0 μM, respectively (Konishi and Watanabe, 1995). However, when the K_d is estimated by a kinetic analysis of the indicator fluorescence change after action potential stimulation, a 2.5-fold higher value (2.5 μM) is obtained (Konishi and Watanabe, 1995). Although the

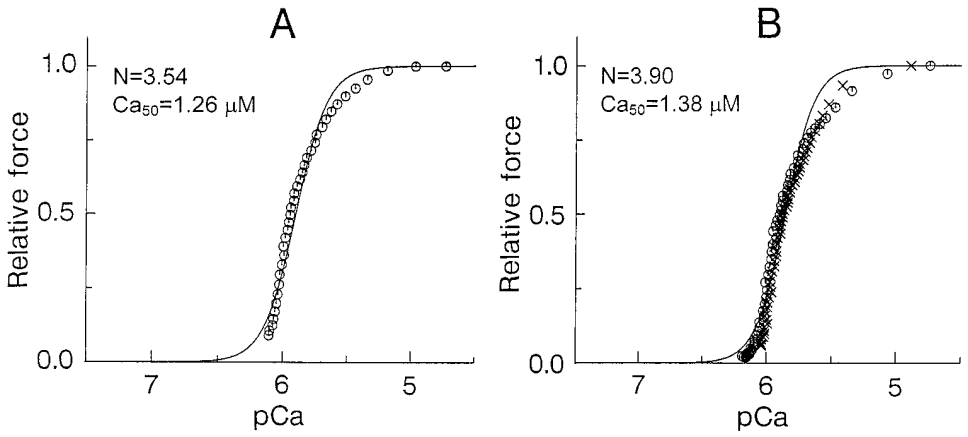

FIGURE 8. Analysis of $[Ca^{2+}]_i$–force relation during the relaxation phase of tetani in the presence of 2 μM TBQ. *A* and *B* were obtained in two different fibers. In *A* and *B*, open circles were sampled at a 200-ms interval from the instantaneous pCa versus force loop as shown in Fig. 6. Each data set was least-squares fitted with the Hill curve (*solid line*) with maximum force level fixed to 1.0 and two adjustable parameters indicated in the panel. In *B*, sampled data at a 500-ms interval from the loop obtained in the presence of 5 μM TBQ are also shown (×). (*A*) Fiber 031095f2, resting sarcomere length 2.7 μm, 70 μM indicator; (*B*) fiber 031595f2, sarcomere length 2.7 μm, 15–14 μM indicator.

kinetic fits may overestimate K_d owing to nonuniform distribution of Ca^{2+} and other uncertainties, it is also possible that permeabilized fibers report erroneously low K_d as a result of the loss of some cytoplasmic molecules (see DISCUSSION in Konishi and Watanabe, 1995). With this second estimate of K_d (2.5 μM), all calculated values of $[Ca^{2+}]_i$ are increased by 2.5-fold; the pCa–force relation presented in Figs. 3, 4, 6, and 8 should be shifted to the right by 0.4 pCa units without any change in the shape of the curves.

Another disadvantage of intact fibers is that intracellular conditions cannot be directly controlled. It is therefore possible that changes of ion concentrations other than $[Ca^{2+}]_i$, such as pH, inorganic phosphate (P_i), and Mg^{2+}, influenced the $[Ca^{2+}]_i$–force relation in intact fibers. For example, Tanokura and Yamada (1984) reported 3.6 mM increase in P_i and alkalization of 0.08 pH units after 5-s tetanic contraction in bullfrog sartorius muscles; these changes could be attributed to the breakdown of creatine phosphate and subsequent protonization of P_i. In the present study, the time integral of contracture force induced by 20 and 30 mM K^+ was, respectively, 3.1 ± 1.0-fold (n = 6) and 8.0 ± 0.4-fold (n = 3) larger than that of 1-s tetanic force. It follows that metabolic changes during the K^+ contractures could be roughly equivalent to those during 3–8-s tetani, and therefore changes of P_i and pH could be similar to those reported in 5-s tetani described above. Alteration of the $[Ca^{2+}]_i$–force relation by such changes of pH and P_i (0.08 and 3.6 mM, respectively) are expected to be small, and no evidence for progressive alteration of Ca^{2+} sensitivity was detected in the instantaneous plot of data during K^+ contractures (Fig. 4).

Time integral of tetanic force in the presence of 1, 2, and 5 μM TBQ was, respectively, 4.3 ± 0.3-fold (n = 11), 8.4 ± 0.7-fold (n = 10), and 31.5 ± 5.6-fold (n = 5) greater than that of 0.5-s tetanic force; metabolic changes at 1, 2, and 5 μM TBQ may be roughly comparable to those of, respectively, 2-, 4-, and 16-s control tetani. Thus, only very prolonged relaxation in the presence of 5 μM TBQ possibly caused the large P_i change and cytoplasmic acidification, owing to lactic acid production, both of which are known to reduce Ca^{2+} sensitivity of myofilaments (Robertson and Kerrick, 1979; Nosek et al., 1990). These metabolic changes might underlie the observed small increase in

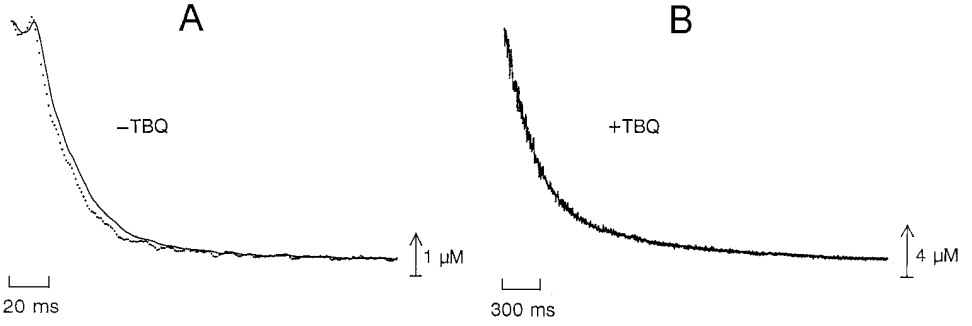

FIGURE 9. Decay of $[Ca^{2+}]_i$ after tetanic stimulation in the absence (*A*) and presence (B) of 2 μM TBQ taken from the experiment shown in Fig. 5. Records start at the last stimulus of the train. In *A* and *B*, solid traces were converted from R signals assuming instantaneous Ca^{2+}-fura dextran reaction, while dotted traces were obtained with kinetic correction for the delay of the reaction (see METHODS).

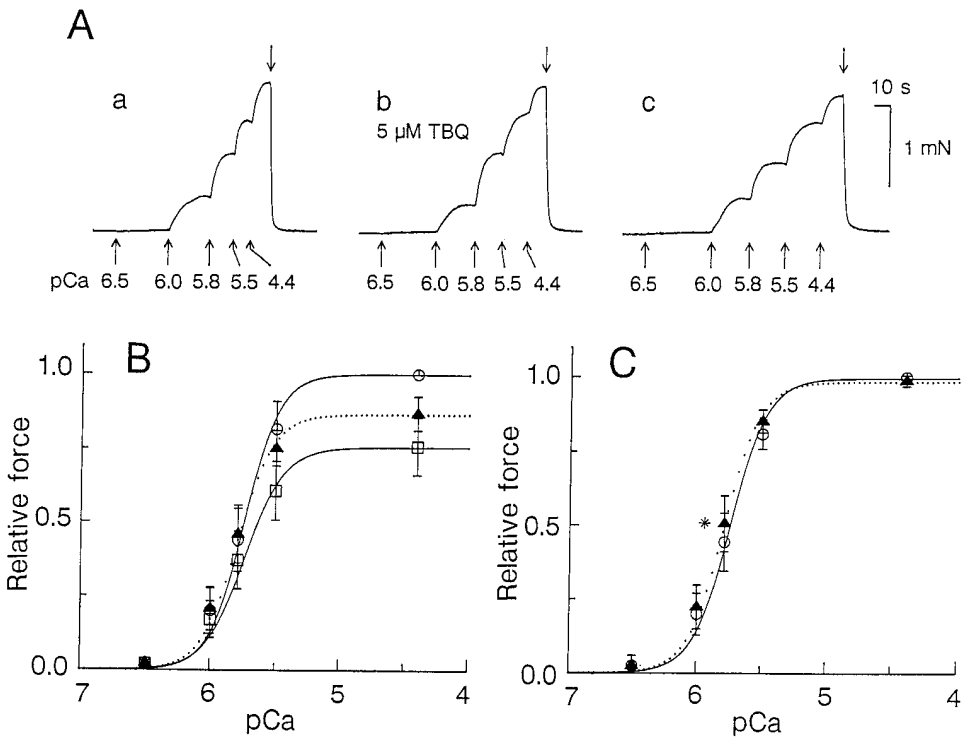

FIGURE 10. (*A*) Ca^{2+}-activated force measurements in a skinned fiber repeated in the absence (*a* and *c*) and presence (*b*) of 5 μM TBQ. The records were taken in a sequence of *a–c* with 15-min intervals. In *a–c*, the bathing solution was changed sequentially from the relaxing solution to solutions of various $[Ca^{2+}]$'s, as indicated in pCa units, and returned back to the relaxing solution (*downward arrow*). In *b*, 5 μM TBQ was applied for 2 min in the relaxing solution, and was maintained throughout the run. Fiber, 042795f4; resting sarcomere length, 2.8 μM. (*B*) Summary of $[Ca^{2+}]$ (pCa units)–force relation obtained as shown in *A* from six skinned fibers; symbols represent means ± SEM of data from the first run in the absence of TBQ (○), from the second run in the presence of 5 μM TBQ (▲), and from the third run after washout of TBQ (□). In each fiber, the steady force levels were normalized to the maximum force (at pCa 4.4) in the first run, and data from each run were fitted to the Hill equation. Smooth curves represent the Hill curve with the average N, Ca_{50}, and $Force_{max}$ from the six fibers; N = 3.25, Ca_{50} = 1.81 μM, $Force_{max}$ = 0.999 for the first run (*solid line*); N = 3.16, Ca_{50} = 1.62 μM, $Force_{max}$ = 0.870 for the second run (*dotted line*); N = 2.87, Ca_{50} = 1.83 μM, $Force_{max}$ = 0.755 for the third run (*solid line*). (*C*) Data from the first and third runs were averaged for each fiber (○, control), and compared with those obtained in the second run (▲, $*P < 0.05$ vs. control). All data points were normalized to the mean maximum force at pCa 4.4 of control. Solid and dotted lines were drawn based on the average N, Ca_{50}, and $Force_{max}$ from the six fibers; N = 3.07, Ca_{50} = 1.81 μM, $Force_{max}$ = 0.996 for control (*solid line*); N = 3.16, Ca_{50} = 1.62 μM, $Force_{max}$ = 0.983 with TBQ (*dotted line*).

Ca_{50} with the increasing TBQ concentration from 2 to 5 μM (Fig. 7 *C*, see also RESULTS).

According to Hou et al. (1991), cytoplasm of frog muscle fibers contains a high concentration of parvalbumin, a Ca^{2+} and Mg^{2+} binding protein (0.76 mM in the tibialis anterior muscle of *Rana temporaria*). As Mg^{2+} is expected to be released from Ca^{2+}–Mg^{2+} binding sites of parvalbumin in exchange with Ca^{2+} (Baylor et al., 1983; Irving et al., 1989), the sustained high $[Ca^{2+}]_i$ levels should cause an elevation of cytoplasmic $[Mg^{2+}]_i$. A gradual increase in $[Mg^{2+}]_i$ would lead to a time-dependent decrease in Ca^{2+} sensitivity, which was not seen in the similar rise and fall in the instantaneous plot during K^+ contractures (Fig. 4). According to Ogawa and Tanokura (1986), dissociation constants of parvalbumin from bullfrogs are estimated to be 0.1–0.17 μM for Ca^{2+} and 1.1–1.2 mM for Mg^{2+} (values for PA1 and PA2, 20°C). If the average values (0.135 μM for Ca^{2+} and 1.15 mM for Mg^{2+}) are used for the dissociation constants, under the assumption of a resting $[Ca^{2+}]_i$ of 60 nM (Konishi and Watanabe, 1995) and $[Mg^{2+}]_i$ of 1.0 mM (Konishi et al., 1993), it can be calculated that 38% of Ca^{2+}–Mg^{2+} binding sites are occupied with Mg^{2+} (and 19% of the sites are occupied with Ca^{2+}) in the resting state. If the frog cytoplasm contains 1.52 mM Ca^{2+}–Mg^{2+} binding sites on 0.76 mM parvalbumin (Hou et al., 1991), at most 0.58 mM Mg^{2+} (1.52 × 0.38) could be released from the sites under very high levels of $[Ca^{2+}]_i$ during activation. Assuming that 37% of the displaced Mg^{2+} will be free and 63% will be bound by other Mg^{2+} buffers such as creatine phosphate (Baylor and Hollingworth, 1988), the increase in $[Mg^{2+}]_i$ would be only 0.22 mM. Thus, the influence of this slight elevation of $[Mg^{2+}]_i$ on the $[Ca^{2+}]_i$–force relation may not be detectable in the experimental data in Fig. 4. Regarding the changes in pH, P_i, and $[Mg^{2+}]_i$, the above consideration, despite a rough approximation with many assumptions involved, suggests that the properties of myofilaments are not modified much in the experimental conditions of the present study.

Analysis of $[Ca^{2+}]_i$–force relation in the present study assumes that sarcomeres within the fibers are homogeneous during activation and relaxation. However, shortening and lengthening of different fiber segments, if this occurs, could reduce overall force production, and consequently could distort the $[Ca^{2+}]_i$–force curve, making the slope of the curve either steeper or shallower depending on which part of the curve was affected. It has been reported that, after tetanic stimulation, sarcomeres remain homogenous dur-

ing the early linear relaxation of force, but become inhomogeneous during the late exponential phase (Huxley and Simmons, 1970). Although we did not estimate the intrafiber sarcomere inhomogeneity, the following considerations suggest that the influence on force measurement may be less extreme in the experimental conditions of the present study, in which relaxation was prolonged by inhibition of SR Ca^{2+} pump. (*a*) The extent of sarcomere inhomogeneity during relaxation is reduced in fatigued frog fibers, where the time course of relaxation of tetanic force is markedly prolonged (Curtin and Edman, 1989). This slow relaxation of tetanic force during fatigue is, at least partly, due to inhibition of SR Ca^{2+} uptake in toad fibers (Westerblad et al., 1997). Thus, slowing the decay of $[Ca^{2+}]_i$ and force after tetani, which was done in the present experiment, might help increase sarcomere uniformity. In fact, in a TBQ-treated *Xenopus* fiber, Westerblad et al. (1997) showed large force recovery after quick release during relaxation, which is similarly seen in a fatigued fiber (see Figs. 6 *B* and 7 *B* in Westerblad et al., 1997). (*b*) The amplitude of nonuniform sarcomere shortening and lengthening has been reported to be smaller at the relatively long resting sarcomere length employed in the present study (2.7–2.8 μM) than at slack length (Edman and Flitney, 1982). (*c*) In the presence of 2 μM TBQ, the $[Ca^{2+}]_i$–force relation during relaxation of tetanic force was similar to that obtained during either the rising or the declining phase of K^+ contractures. It seems difficult to reconcile this similarity with a large influence of inhomogeneous sarcomeres unless it is assumed that these different types of activation and relaxation experienced similar influence of sarcomere nonuniformity. To resolve the problem concerning the sarcomere shortening and lengthening, however, it would be necessary to do experiments with careful control of sarcomere length, while $[Ca^{2+}]_i$ and force are simultaneously measured.

Comparison of $[Ca^{2+}]_i$–Force Curves Reported with Other Techniques

Results of the present study gave estimates for N of 3.2–3.9 and Ca_{50} of ~1.6 μM (Table I). The latter value could be as high as 4.0 μM (1.6 μM × 2.5), if a higher estimate of the indicator K_d was used (see above). These values may be compared with previously reported values in intact amphibian skeletal muscles.

Allen et al. (1989) estimated the $[Ca^{2+}]_i$–force relation in *Xenopus* muscle fibers with aequorin as a Ca^{2+} indicator (21°C). Their data are consistent with N and Ca_{50} values of 3.0–3.7 and 2.4–3.0 μM (see DISCUSSION in Maughan et al., 1995). These values of N and Ca_{50} are within the similar range as those obtained in the present study, although Allen et al. (1989) acknowledged possible weaknesses of the aequorin calibration procedure, and basically used their results as an indication rather than a precise calibration of $[Ca^{2+}]_i$.

In a series of experiments with indo-1 in type 2 (fast twitch) fibers from *Xenopus* skeletal muscle fibers, Westerblad and Allen (1996) and Westerblad et al. (1997) constructed the $[Ca^{2+}]_i$–force curve using normal tetani and tetani during postcontractile depression after recovery from fatigue. The curves gave an N value of 4.1 and Ca_{50} values of 0.59–0.65 μM (sarcomere length ~2.3 μm, 22°C). The slope of the relation (N) is similar to those obtained in the present study from frog (*Rana temporaria*) muscle fibers (3.2–3.9, Table I). The Ca_{50} values are lower by a factor of 2.6–6.5 than those estimated by us (1.6–4.0 μM, Table I; also see above). The discrepancy may be smaller than is apparent if Ca_{50} values are inversely related to experimental temperature; Maughan et al. (1995) reported that lowering the temperature from 22 to 16°C caused a 78% increase in Ca_{50} in frog skinned fibers bathed in solutions that mimicked most known cytoplasmic ion constituents, although earlier skinned fiber studies reported temperature-dependent changes of Ca_{50} in the opposite direction (Godt and Lindley, 1982; Stephenson and Williams, 1985). On the other hand, lengthening the fiber to a longer sarcomere length in the present study (2.7–2.8 μm) should decrease Ca_{50} (Endo, 1972; Moisescu and Thieleczek, 1979; Martyn et al., 1993). The remaining discrepancy of Ca_{50} values could reflect the difficulties in calibrating indicator Ca^{2+} signals in terms of $[Ca^{2+}]_i$ (see above). Maximal $[Ca^{2+}]_i$ level reached during the plateau phase of tetanic force was ~2 μM in Westerblad and Allen (1996) and Westerblad et al. (1997), whereas it was 8.3–20.7 μM, depending on the choice of the indicator K_d, in the present study (average values from 11 control tetani stimulated at 100 Hz for 0.5 s). Our high estimates of $[Ca^{2+}]_i$ levels obtained during high frequency tetani are consistent with large Ca^{2+} transients with a peak amplitude of 10–17 μM, previously detected during twitch in frog fibers with furaptra, a low affinity Ca^{2+} indicator that is likely to supply relatively accurate information about the amplitude of Ca^{2+} transients (Konishi et al., 1991; Zhao et al., 1996). It is also possible, however, that a true difference in the $[Ca^{2+}]_i$–force relation exists between toad and frog fibers.

Morgan et al. (1997), using acetoxy-methyl (AM)-loaded fura-2 in single fibers of *Rana temporaria* (sarcomere length ~2.2 μm, 3°C), recently estimated that the average value of N was at least 15, and could be as high as 25. This extremely steep relation between $[Ca^{2+}]_i$ and force is in sharp contrast with the present results and other results (above). The large discrepancy in N values does not appear to be explained by the small effects of different experimental temperatures and sarcomere length on the slope (N) reported in

skinned fibers (Moisescu and Thieleczek, 1979; Godt and Lindley, 1982; Stephenson and Williams, 1985; Martyn et al., 1993; Maughan et al., 1995). Rather, the discrepancy might be caused by errors in calibration of indicator signals in one or more of the above studies; errors in estimates of R_1 (R_{max}) or R_0 (R_{min}), or both, but not K_d, could produce significant errors in estimation of N. For the indicators introduced with their AM ester forms, indicator molecules may not be completely deesterified or may not be located entirely within cytoplasm. Morgan et al. (1997) found that 20–50% of fluorescence from AM-loaded frog fibers was not removed by cell membrane permeabilization with saponin, suggesting that a substantial fraction of fura-2 molecules were either tightly bound to some structures or trapped inside some organelles. Although Morgan et al. (1997) have corrected their results for several estimates of possible errors that arose from these "$[Ca^{2+}]_i$-unrelated" indicator signals, the high N value of 15–25 might be attributed to incomplete correction for the $[Ca^{2+}]_i$-unrelated signals. It has been reported that the $[Ca^{2+}]_i$-unrelated component of AM-loaded indicators would present a significant source of error in the estimation of $[Ca^{2+}]_i$, particularly when the loaded concentration is small (Zhao et al., 1997).

Comparison with Skinned Fiber Results

In the present study, the $[Ca^{2+}]_i$–force relation was also obtained in skinned fibers with many of the important experimental conditions matched to those for intact fibers. The estimated N and Ca_{50} values from skinned fibers were similar to those estimated from intact fibers (Table I). Similarity of Ca_{50} values between intact and skinned fibers may be somewhat fortuitous because exact positioning of the pCa–force curve of skinned fibers is influenced by factors other than sarcomere length and temperature (e.g., pH, ionic strength, etc.; see Fink et al., 1986). Close agreement of N, however, indicates similar steepness of the $[Ca^{2+}]_i$–force relation in intact and skinned fibers, and does not provide any evidence for altered myofilament cooperativity due to the skinning procedure in fast twitch muscle of frogs. The present observation stands in contrast to the reported decrease in the slope by skinning in rat cardiac muscle (Gao et al., 1994). It is not clear at this point, however, whether the different results obtained from frog skeletal muscle and rat cardiac muscle truly reflect the tissue and species differences.

Maughan et al. (1995) measured the $[Ca^{2+}]$–force relation in frog skinned fibers, using the bathing solutions that they proposed to best mimic the normal cytoplasm of intact muscle fibers (Godt and Maughan, 1988). Their estimates of N and Ca_{50} values were 4.85 and 2.58 μM at 16°C, pH 7.25, and a sarcomere length of 2.0 μm. Cytoplasmic pH (pH_i) of intact frog fibers has been reported previously from measurements with pH-sensitive microelectrodes. From the relation between pH_i and pH of HEPES-buffered extracellular solution reported by Curtin (1986), a pH_i value of ~6.9–7.0 might be expected under the conditions of our experiments. The Ca_{50} value obtained by Maughan et al. (1995) would be somewhat larger if their solution pH was set lower by 0.25–0.35 to approximate pH_i of the present experiment; Robertson and Kerrick (1979) reported that decreasing pH from 7.5 to 7.0 increased Ca_{50} by 86% (−0.27 pCa units) in skinned fibers from frogs. The increase in Ca_{50} for a pH of 0.25−0.35 lower, which is expected to be smaller than 86%, would be partially canceled by the opposing effect of the longer sarcomere length in the present study, 2.7–2.8 μm, compared with 2.0 μm (Maughan et al., 1995); Martyn et al. (1993) found that sarcomere lengthening from 2.4 to 3.1 μm decreased Ca_{50} by 32% (+0.17 pCa) in skinned frog fibers. Thus, with corrections for some differences in pH and sarcomere length, the Ca_{50} value estimated by Maughan et al. (1995) is likely to be within the range of, and be consistent with, our estimate (1.6–4.0 μM). Our N values (3.2–3.9, Table I), slightly smaller than the value (4.85) reported by Maughan et al. (1995), could also be attributed to stretch-induced shallowing of the slope observed in skinned fibers (Endo, 1972; Martyn et al., 1993).

Range of $[Ca^{2+}]_i$ Required for Active Force Development

With N and Ca_{50} values obtained during K^+ contracture (3.92 and 1.69–4.23 μM, respectively), our measurements imply that the isometric force is minimally activated (5% level of the maximum force) by a 13-fold increase in $[Ca^{2+}]_i$, and it is nearly saturated (95% level of maximum force) by a 60-fold increase in $[Ca^{2+}]_i$ from the resting level, independent of the choice of the indicator K_d. The results thus suggest that a $[Ca^{2+}]_i$ change by a factor of 4.5 (or 0.65 pCa units) is required to bring myofilaments from threshold activation to nearly full activation, allowing graded control of isometric force by $[Ca^{2+}]_i$ of a relatively wide range. The present results, however, do not contradict the myosin–Ca^{2+} cooperativity hypothesis, the cooperative binding of Ca^{2+} to neighboring troponin C molecules induced by cross-bridge attachment, as a Hill coefficient of 3–4 is clearly larger than expected from independent Ca^{2+} binding to troponin C, which only has two low affinity Ca^{2+} binding sites.

We thank S. Kurihara for his helpful discussion during the course of this work and for instructions on making high K^+ solutions, and M. Sibuya for reading the manuscript.

This work was supported by a Grant-in-Aid for Scientific Research from the Ministry of Education, Science and Culture, Tokyo, Japan.

Original version received 9 December 1997 and accepted version received 21 January 1998.

REFERENCES

Allen, D.G., J.A. Lee, and H. Westerblad. 1989. Intracellular calcium and tension during fatigue in isolated single muscle fibres from *Xenopus laevis*. *J. Physiol. (Camb.)*. 415:433–458.

Baker, A.J., R. Brandes, J.H.M. Schreur, S.A. Camacho, and M.W. Wiener. 1994. Protein and acidosis alter calcium-binding and fluorescence spectra of the calcium indicator indo-1. *Biophys. J.* 67: 1646–1654.

Bakker, A.J., G.D. Lamb, and D.G. Stephenson. 1992. The effect of 2,5-di(*tert*-butyl)-1,4-benzohydroquinone on the contractile apparatus and depolarization-induced contraction in skinned muscle fibres of the toad. *Proc. Aust. Physiol. Pharmacol. Soc.* 23:150P. (Abstr.)

Baylor, S.M., W.K. Chandler, and M.W. Marshall. 1983. Sarcoplasmic reticulum calcium release in frog skeletal muscle fibres estimated from arsenazo III calcium transients. *J. Physiol. (Camb.)*. 344:625–666.

Baylor, S.M., and S. Hollingworth. 1988. Fura-2 calcium transients in frog skeletal muscle fibres. *J. Physiol. (Camb.)*. 403:151–192.

Beeler, T.J., A. Schibeci, and A. Martonosi. 1980. The binding of arsenazao III to cell components. *Biochim. Biophys. Acta*. 629:317–327.

Cannell, M.B. 1986. Effect of tetanus duration on the free calcium during the relaxation of frog skeletal muscle fibres. *J. Physiol. (Camb.)*. 376:203–218.

Caputo, C., K.A.P. Edman, F. Lou, and Y.-B. Sun. 1994. Variation in myoplasmic Ca^{2+} concentration during contraction and relaxation studied by the indicator fluo-3 in frog muscle fibres. *J. Physiol. (Camb.)*. 478:137–148.

Curtin, N.A. 1986. Buffer power and intracellular pH of frog sartorius muscle. *Biophys. J.* 50:837–841.

Curtin, N.A., and K.A.P. Edman. 1989. Effects of fatigue and reduced intracellular pH on segment dynamics in 'isometric' relaxation of frog muscle fibres. *J. Physiol. (Camb.)*. 413:159–174.

Edman, K.A.P., and F.W. Flitney. 1982. Laser diffraction studies of sarcomere dynamics during 'isometric' relaxation in isolated muscle fibres of the frog. *J. Physiol. (Camb.)*. 329:1–20.

Endo, M. 1972. Stretch-induced increase in activation of skinned muscle fibres by calcium. *Nat. New Biol.* 237:211–213.

Endo, M., and M. Iino. 1980. Specific perforation of muscle cell membranes with preserved SR functions by saponin treatment. *J. Muscle Res. Cell Motil.* 1:89–100.

Fink, R.H.A., D.G. Stephenson, and D.A. Williams. 1986. Potassium and ionic strength effects on the isometric force of skinned twitch muscle fibres of the rat and toad. *J. Physiol. (Camb.)*. 370: 317–337.

Gao, W.D., P.H. Backx, M. Azan-Backx, and E. Marban. 1994. Myofilament Ca^{2+} sensitivity in intact versus skinned rat ventricular muscle. *Circ. Res.* 74:408–415.

Godt, R.E., and B.D. Lindley. 1982. Influence of temperature upon contractile activation and isometric force production in mechanically skinned muscle fibers of the frog. *J. Gen. Physiol.* 80:279–297.

Godt, R.E., and D.W. Maughan. 1988. On the composition of the cytosol of relaxed skeletal muscle of the frog. *Am. J. Physiol.* 254: C591–C604.

Horiuti, K., H. Higuchi, Y. Umazume, M. Konishi, O. Okazaki, and S. Kurihara. 1988. Mechanism of action of 2,3-butanedione 2-monoxime on contraction of frog skeletal muscle fibres. *J. Muscle Res. Cell Motil.* 9:156–164.

Hou, T.-T., J.D. Johnson, and J.A. Rall. 1991. Parvalbumin content and Ca^{2+} and Mg^{2+} dissociation rates correlated with changes in relaxation rate of frog muscle fibres. *J. Physiol. (Camb.)*. 441:285–304.

Huxley, A.F., and R.M. Simmons. 1970. Rapid 'give' and the tension 'shoulder' in the relaxation of frog muscle fibres. *J. Physiol. (Camb.)*. 210:32P–33P. (Abstr.)

Huxley, A.F., and L.D. Peachy. 1961. The maximum length for contraction in vertebrate striated muscle. *J. Physiol. (Camb.)*. 156:150–165.

Irving, M., J. Maylie, N.L. Sizto, and W.K. Chandler. 1989. Simultaneous monitoring of changes in magnesium and calcium concentrations in frog cut twitch fibers containing antipyrylazo III. *J. Gen. Physiol.* 93:585–608.

Konishi, M., S. Hollingworth, A.B. Harkins, and S.M. Baylor. 1991. Myoplasmic calcium transients in intact frog skeletal muscle fibers monitored with the fluorescent indicator furaptra. *J. Gen. Physiol.* 97:271–301.

Konishi, M., A. Olson, S. Hollingworth, and S.M. Baylor. 1988. Myoplasmic binding of fura-2 investigated by steady-state fluorescence and absorbance measurements. *Biophys. J.* 54:1089–1104.

Konishi, M., N. Suda, and S. Kurihara. 1993. Fluorescence signals from the Mg^{2+}/Ca^{2+} indicator furaptra in frog skeletal muscle fibers. *Biophys. J.* 64:223–239.

Konishi, M., and M. Watanabe. 1995. Resting cytoplasmic free Ca^{2+} concentration in frog skeletal muscle measured with fura-2 conjugated to high molecular weight dextran. *J. Gen. Physiol.* 106: 1123–1150.

Kurebayashi, N., A.B. Harkins, and S.M. Baylor. 1993. Use of fura red as an intracellular calcium indicator in frog skeletal muscle fibers. *Biophys. J.* 64:1934–1960.

Lee, J.A., H. Westerblad, and D.G. Allen. 1991. Changes in tetanic and resting $[Ca^{2+}]_i$ during fatigue and recovery of single muscle fibres from *Xenopus laevis*. *J. Physiol. (Camb.)*. 433:307–326.

Lüttgau, H.Ch., and W. Spiecker. 1979. The effects of calcium deprivation upon mechanical and electrophysiological parameters in skeletal muscle fibres of the frog. *J. Physiol. (Camb.)*. 296:411–429.

Martell, A.E., and R.M. Smith. 1974. Critical Stability Constants. Vol. 1. Amino Acids. Plenum Publishing Corp., New York, NY.

Martyn, D.A., R. Coby, L.L. Huntsman, and A.M. Gordon. 1993. Force-calcium relations in skinned twitch and slow-tonic frog muscle fibres have similar sarcomere length dependencies. *J. Muscle Res. Cell Motil.* 14:65–75.

Maughan, D.W., J.E. Molloy, M.A.P. Brotto, and R.E. Godt. 1995. Approximating the isometric force-calcium relation of intact frog muscle using skinned fibers. *Biophys. J.* 69:1484–1490.

Moisescu, D.G., and R. Thieleczek. 1979. Sarcomere length effects on the Sr^{2+}- and Ca^{2+}-activation curves in skinned frog muscle fibres. *Biochim. Biophys. Acta*. 546:64–76.

Morgan, D.L., D.R. Claflin, and F.J. Julian. 1997. The relationship between tension and slowly varying intracellular calcium concen-

tration in intact frog skeletal muscle. *J. Physiol. (Camb.).* 500:177–192.

Natori, R. 1954. The role of myofibrils, sarcoplasma and sarcolemma in muscle-contraction. *Jikeikai Med. J.* 1:18–28.

Nosek, T.M., J.H. Leal-Cardoso, M. McLaughlin, and R.E. Godt. 1990. Inhibitory influence of phosphate and arsenate on contraction of skinned skeletal and cardiac muscle. *Am. J. Physiol.* 259: C933–C939.

Ogawa, Y., and M. Tanokura. 1986. Steady-state properties of calcium binding to parvalbumins from bullfrog skeletal muscle: effects of Mg^{2+}, pH, ionic strength, and temperature. *J. Biochem.* 99: 73–80.

Okazaki, O., N. Suda, K. Hongo, M. Konishi, and S. Kurihara. 1990. Modulation of Ca^{2+} transients and contractile properties by β-adrenoceptor stimulation in ferret ventricular muscles. *J. Physiol. (Camb.).* 423:221–240.

Robertson, S.P., and W.G.L. Kerrick. 1979. The effects of pH on Ca^{2+}-activated force in frog skeletal muscle fibers. *Pflügers Arch.* 380:41–45.

Stephenson, D.G., and D.A. Williams. 1985. Temperature-dependent calcium sensitivity changes in skinned muscle fibres of rat and toad. *J. Physiol. (Camb.).* 360:1–12.

Tanokura, M., and K. Yamada. 1984. Changes in intracellular pH and inorganic phosphate concentration during and after muscle contraction as studied by time-resolved ^{31}P-NMR. *FEBS Lett.* 171: 165–168.

Westerblad, H., and D.G. Allen. 1993. The influence of intracellular pH on contraction, relaxation and $[Ca^{2+}]_i$ in intact single fibres from mouse muscle. *J. Physiol. (Camb.).* 466:611–628.

Westerblad, H., and D.G. Allen. 1994. The role of sarcoplasmic reticulum in relaxation of mouse muscle: effects of 2,5-di(*tert*-butyl)-1,4-benzohydroquinone. *J. Physiol. (Camb.).* 474:291–301.

Westerblad, H., and D.G. Allen. 1996. Slowing of relaxation and $[Ca^{2+}]_i$ during prolonged tetanic stimulation of single fibres from *Xenopus* skeletal muscle. *J. Physiol. (Camb.).* 492:723–736.

Westerblad, H., J. Lännergren, and D.G. Allen. 1997. Slowed relaxation in fatigued skeletal muscle fibers of *Xenopus* and mouse. Contribution of $[Ca^{2+}]_i$ and cross-bridges. *J. Gen. Physiol.* 109: 385–399.

Yue, D.T., E. Marban, and W.G. Wier. 1986. Relationship between force and intracellular $[Ca^{2+}]$ in tetanized mammalian heart muscle. *J. Gen. Physiol.* 87:223–242.

Zhao, M., S. Hollingworth, and S.M. Baylor. 1996. Properties of tri- and tetracarboxylate Ca^{2+} indicators in frog skeletal muscle fibers. *Biophys. J.* 70:896–916.

Zhao, M., S. Hollingworth, and S.M. Baylor. 1997. AM-loading of fluorescent Ca^{2+} indicators into intact single fibers of frog muscle. *Biophys. J.* 72:2736–2747.